

tion of the coordinated  $N_2$  with  $H_2$  in the presence of **2**. Although the detailed reaction mechanism for the formation of  $NH_3$  is not yet clear, the first step must be the direct reaction of the  $N_2$  complex **3** with the  $H_2$  complexes **1** to form hydrazido(2-) complexes. In this reaction, the heterolytic cleavage of  $H_2$  occurs at the Ru center, where one H atom is used for protonation of the coordinated  $N_2$  on the W atom and the other H atom remains at the Ru atom as a hydride. Further protonation of the hydrazido(2-) complexes with the  $H_2$  complexes **1** results in the formation of  $NH_3$ . Because **3** is synthesized under 1 atm of  $N_2$  at ambient temperature, the present reaction allows the formation of  $NH_3$  directly from  $N_2$  and  $H_2$  under mild conditions.

Interestingly, when **3** was treated in the presence of acetone with an equilibrium mixture derived from 10 equiv of **2a**, **2b**, or **2c** under 1 atm of  $H_2$  at 55°C for 24 hours, acetone azine was formed in 65, 80, or 100% yield based on the W atom, respectively (Scheme 3). The yield of acetone azine depended on the nature of the counteranion of

**2**. The formation of acetone azine was not observed without  $H_2$ . However, when complex **6** was used instead of complex **3**, the diazoalkane complexes *trans*-[WF(NNCMe<sub>2</sub>)(dpppe)<sub>2</sub>]X [X = PF<sub>6</sub> (**8a**); X = BF<sub>4</sub> (**8b**)] were formed in high yields. Complex **8b** has been isolated and characterized by spectroscopy. The same complexes are well known to be derived from the condensation of *trans*-[WF(NNH<sub>2</sub>)(dpppe)<sub>2</sub>]X with acetone (**13**). The formation of acetone azine has previously been observed upon treatment of **3** with a methanol-acetone mixture at 50°C (**14**). We believe that the mechanism of the present reaction is essentially similar to the previous one, which includes a diazoalkane complex as an intermediate. However, it is noteworthy that  $H_2$  can be used in place of methanol.

## REFERENCES AND NOTES

1. G. Ertl, in *Catalytic Ammonia Synthesis*, J. R. Jennings, Ed. (Plenum, New York, 1991).
2. For a recent review, see M. Hidai and Y. Mizobe, *Chem. Rev.* **95**, 1115 (1995).
3. M. Hidai, K. Tominari, Y. Uchida, A. Misono, *Chem. Commun.* **1969**, 1392 (1969).
4. J. Chatt, A. J. Pearson, R. L. Richards, *J. Chem. Soc.*

- Dalton Trans.* **1977**, 1852 (1977); T. Takahashi *et al.*, *J. Am. Chem. Soc.* **102**, 7461 (1980).
5. M. Hidai, K. Tominari, Y. Uchida, *J. Am. Chem. Soc.* **94**, 110 (1972); T. A. George and R. C. Tisdale, *Inorg. Chem.* **27**, 2909 (1988).
6. M. Hidai *et al.*, *Chem. Lett.* **1980**, 645 (1980); T. Saito *et al.*, *J. Am. Chem. Soc.* **104**, 4367 (1982).
7. G. Jia, R. H. Morris, C. T. Schweitzer, *Inorg. Chem.* **30**, 594 (1991).
8. M. D. Fryzuk *et al.*, *Science* **275**, 1445 (1997).
9. Y. Ishii, Y. Ishino, T. Aoki, M. Hidai, *J. Am. Chem. Soc.* **114**, 5429 (1992); Y. Ishii, M. Kawaguchi, Y. Ishino, T. Aoki, M. Hidai, *Organometallics* **13**, 5062 (1994); M. Hidai *et al.*, *Chem. Lett.* **1991**, 383 (1991).
10. A. Mezzetti *et al.*, *Inorg. Chem.* **36**, 711 (1997).
11. Y. Nishibayashi, S. Iwai, M. Hidai, unpublished results.
12. J. Chatt, G. A. Heath, R. L. Richards, *J. Chem. Soc. Dalton Trans.* **1974**, 2074 (1974); M. Hidai *et al.*, *Inorg. Chem.* **15**, 2694 (1976).
13. M. Hidai, Y. Mizobe, M. Sato, T. Kodama, Y. Uchida, *J. Am. Chem. Soc.* **100**, 5740 (1978); Y. Mizobe, Y. Uchida, M. Hidai, *Bull. Chem. Soc. Jpn.* **53**, 1781 (1980); P. C. Bevan, J. Chatt, M. Hidai, J. Leigh, *J. Organomet. Chem.* **160**, 165 (1978).
14. M. Hidai *et al.*, *J. Organomet. Chem.* **254**, 75 (1983).
15. Supported by a Grant-in-Aid for Specially Promoted Research (09102004) from the Ministry of Education, Science, Sports, and Culture, Japan. This paper is part 54 of Preparation and Properties of Molybdenum and Tungsten Dinitrogen Complexes.

27 October 1997; accepted 25 November 1997

## Isolation of an Intrinsic Precursor to Molecular Chemisorption

David E. Brown, Douglas J. Moffatt, Robert A. Wolkow\*

Over the past 70 years, numerous gas-surface adsorption studies have indicated the existence of a weakly bound, mobile intermediate that is a precursor to chemical bond formation. The direct observation and characterization of such a species are presented. Precursor and chemisorbed benzene on a silicon surface were clearly distinguished with the use of a tunable-temperature scanning tunneling microscope. Precursor decay to chemisorption was observed, allowing the salient features of the potential energy surface to be determined.

The microscopic details of gas-surface adsorption dynamics have been actively studied for the better part of a century. Much of the conceptual framework in use today builds upon the pioneering work of Langmuir (1) and Lennard-Jones (2), who studied the nature of forces acting when atomic or molecular species come into contact with a surface. Although knowledge of physical interactions between adsorbates and surfaces (physisorption) and of relatively strong chemical interactions (chemisorption) has advanced steadily over the years, important issues remain to be addressed. One such issue, central to a discussion of adsorption phenomena and a recurring theme throughout the history of

surface science, involves an adsorption intermediate known as a precursor. Although no direct observation or characterization has been achieved, numerous observations consistent with precursor-mediated adsorption have led to widespread use of the concept (3). Here, we describe the direct observation of this evasive but likely common entity.

In Langmuir's early work, a simple scenario was considered in which an impinging species either was chemisorbed when striking an adsorbate-free surface site or was scattered back into the gas phase upon encountering an occupied site, leading to a linear dependence of the sticking coefficient (that is, the probability of adsorbing) on surface coverage. Exceptions to this behavior—systems exhibiting near-unity sticking probability at high coverage—were noted early on, for example, Cs (4) and  $N_2$  (5) adsorption on tungsten. To account for these observations, more sophis-

ticated models by Morrison and Roberts (6) and Kisliuk (7) invoked a weakly bound, mobile intermediate state that allowed incoming adsorbates to search for a free site. Later adsorption studies, usually measurements of sticking coefficients (8–10), pointed to such a precursor-mediated adsorption mechanism (3). Numerous theoretical papers have modeled the role of precursor states in adsorption and desorption (11, 12). A notable advance came with the work of Doren and Tully, who pointed out that rather the free energy of interaction, not only the enthalpy, should be considered in understanding precursors (11).

Two very different types of precursor have been described. The extrinsic precursor is associated with incoming molecules blocked from direct chemisorption by preexisting adsorbed molecules. It is weakly bound to an adsorbate-covered portion of the surface through van der Waals interactions but is free to diffuse laterally, increasing the opportunity to find a free site for chemisorption. Our focus is on the intrinsic precursor, a physisorbed intermediate state that does not arise from simple blocking of adsorption sites. Rather, it exists spatially at virtually the same point where chemisorption can occur, but is inhibited from forming a stronger bond by a barrier related to the structural distortion or realignment of the molecule, the surface, or both. The intrinsic precursor is thought to be physisorbed and laterally free-moving, like the extrinsic precursor. Although they are fundamentally different entities, both precursor types are described by the schematic po-

National Research Council of Canada (NRCC), Steacie Institute for Molecular Sciences, 100 Sussex Drive, Ottawa, Ontario K1A 0R6, Canada.

\*To whom correspondence should be addressed.

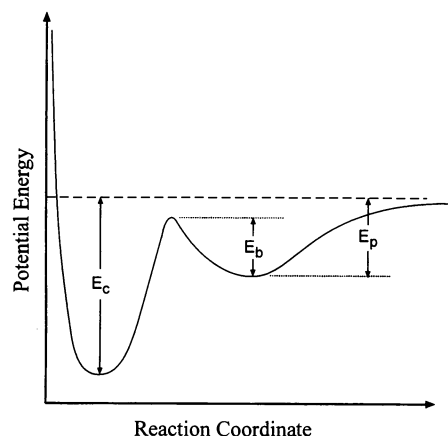


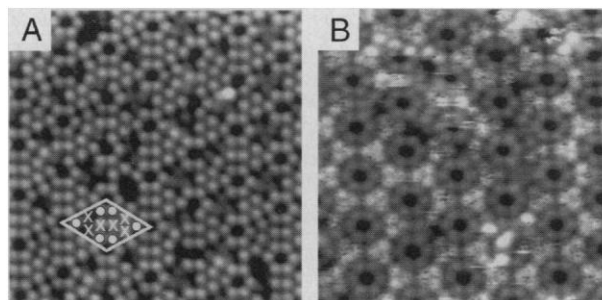
**Fig. 1.** Schematic potential energy diagram describing precursor-mediated adsorption.  $E_p$  and  $E_c$  are the well depths for physisorption and chemisorption, respectively.  $E_b$  is the barrier controlling precursor decay to chemisorption.

tential energy curve in Fig. 1.

We have studied benzene molecules adsorbed on a silicon(111) surface. The (111) facet of silicon, upon cleaning and annealing, spontaneously forms what is known as a  $7\times 7$  reconstructed surface (13). Each surface atom in this structure is three-coordinate with one dangling bond directed normal to the surface plane. The spacing between the topmost atoms, known as adatoms, is  $7.7 \text{ \AA}$  (14). A simple molecular model indicates that one benzene molecule oriented parallel to the surface can be accommodated per silicon adatom. Several studies of benzene adsorption on Si(111)- $7\times 7$  have been undertaken (15–19). Thermal desorption spectrometry (TDS) (16, 18) and electron energy loss spectroscopy (EELS, a surface vibration spectroscopy) (18) studies have shown that benzene adsorbs molecularly on the Si(111)- $7\times 7$  surface at room temperature. EELS spectra showed features attributed to both physisorbed and chemisorbed benzene below  $\sim 150 \text{ K}$  (18). However, only features arising from chemisorbed benzene were observed at room temperature. The relative EELS loss-peak intensities of the benzene vibrational modes having dynamic dipole moments parallel to the ring indicate that the benzene molecule is oriented with the molecular plane parallel to the silicon surface (18). The TDS results are consistent with a relatively weak  $\pi$ -bonding interaction between the silicon adatom dangling bond and the delocalized  $\pi$  network of the benzene molecule as opposed to a strong  $\sigma$ -bond, also indicating that the plane of the chemisorbed molecule is parallel to the silicon surface plane (18). Numerous experimental investigations of benzene adsorption on transition metals have also found this bonding geometry (9, 10, 20).

An ultrahigh-vacuum chamber was used to prepare and maintain extremely clean sil-

**Fig. 2.** (A) STM image recorded at 120 K of benzene adsorbed on Si(111)- $7\times 7$  at a coverage of  $\sim 0.2$  monolayer. The white protrusions are silicon adatoms. The white diamond shape marks a single  $7\times 7$  unit cell. In the absence of benzene, each unit cell would exhibit 12 adatoms. We differentiate between the six center adatoms, marked with X's, and the six corner adatoms, marked with white circles. Darkened adatom sites have benzene molecules chemisorbed.  $V_{\text{sample}} = +1.5 \text{ V}$ , current =  $0.1 \text{ nA}$ ,  $140 \times 140 \text{ \AA}$ . (B) STM image of benzene on Si(111)- $7\times 7$  at 78 K at a coverage of  $\sim 0.5$  monolayer. The precursors appear as protrusions positioned over the center adatoms.  $V_{\text{sample}} = +1.5 \text{ V}$ , current =  $0.1 \text{ nA}$ ,  $140 \times 140 \text{ \AA}$ .



icon surfaces, which were investigated using a tunable-temperature cryogenic scanning tunneling microscope (STM) (19, 21). By operating at cryogenic temperatures, the STM can freeze out kinetically controlled processes or allow them to proceed at a convenient rate. The topography that the STM senses is influenced both by the position of atoms and by local electronic structure. As in previous studies of chemisorption on the  $7\times 7$  surface, the chemisorbed benzene molecule is signaled by a “darkened” site (topographically lower with respect to a clean silicon atom) because of quenching of the silicon dangling bond state and because adsorbed benzene has small state density in the energy window probed (22).

STM images of Si(111)- $7\times 7$  surfaces with  $\sim 20\%$  surface sites covered by benzene molecules (23) recorded at temperatures in the range  $\sim 100$  to  $300 \text{ K}$  (Fig. 2A) are indistinguishable. Benzene molecules are seen as darkened sites, consistent with a chemisorbed state. Strikingly different images result when the experiment is carried out with a surface maintained at  $78 \text{ K}$  (Fig. 2B). Adsorbed benzene molecules now appear as prominent protrusions (24). Because this state is only observed at low temperature, we identify it as the physisorbed state indicated in thermal desorption measurements (16, 18). Although observation of a physisorbed state is not in itself remarkable, this particular physisorbed state is remarkable in that the molecules exist spatially over a site where relatively strong

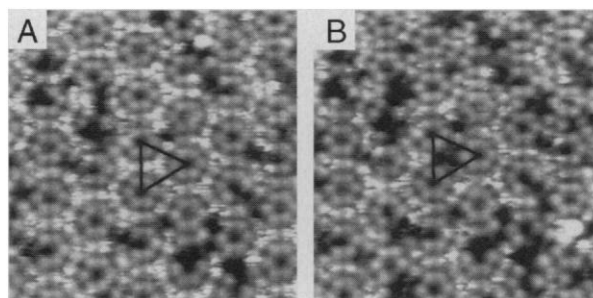
chemical adsorption can (and in time will) occur. By changing only the substrate temperature, a different adsorbed molecular state has been prepared. This state is an intrinsic precursor to chemisorption.

Sequences of images recorded at  $78 \text{ K}$  reveal decay of some precursor molecules to the chemisorption state. Very few events were observed (during observation times of  $\sim 2$  hours), but enough have been recorded to extract an estimate of the barrier separating the precursor from the chemisorbed state. Assuming a preexponential of  $10^{13} \text{ s}^{-1}$ , this barrier is  $E_b \sim 0.3 \text{ eV}$ .

At  $95 \text{ K}$ , the chemisorbed state is dominant. However, immediately after dosing, relatively faint speckled features similar to those observed at  $78 \text{ K}$  were seen. These features were transient; on a time scale of several minutes, these features became increasingly faint and then invisible. Coinciding with the disappearance of the precursor molecules, new features attributable to chemisorbed benzene were observed in the same immediate vicinity. These features represent benzene molecules decaying from the precursor to the chemisorbed state.

To better study the kinetics of precursor decay, we have used an electric field effect to prepare the precursor state at will. We have found that the electric field in the immediate vicinity of the STM tip can be used to place molecules in the precursor state by dislodging chemisorbed molecules. Related field-driven processes have been described previously

**Fig. 3.** Decay of the precursor state at  $95 \text{ K}$ . The precursor state was prepared using the tip electric field. (A) Immediately after preparing the precursor state. (B) After 7 min, a reduction in the number of precursor molecules is observed. The triangular region marks one area where precursor decay to the chemisorbed state has occurred. Careful inspection reveals numerous other examples.  $V_{\text{sample}} = +1.5 \text{ V}$ , current =  $0.1 \text{ nA}$ ,  $140 \times 140 \text{ \AA}$ .



(25). Scanning conditions may be set either for imaging, with virtually no disruption of the molecule-surface complex, or for dislodging of the chemisorbed molecules within the vicinity of the tip (typically  $-3$  V sample bias,  $0.1$  nA). Chemisorbed benzene molecules can be dislodged at any of the temperatures studied. From room temperature down to  $\sim 150$  K, molecules disrupted in this way cannot be observed as they move laterally or desorb from the surface. However, below  $\sim 100$  K, the benzene molecules are trapped long enough to be visible with the STM.

Precursor molecules were prepared using the above method, at a substrate temperature of  $95$  K. Through a time sequence of images, the kinetics of the decay to the precursor state have been monitored. The first image in the sequence is shown in Fig. 3A. The image recorded  $\sim 7$  min later (Fig. 3B) reveals that some benzene molecules have converted back to the dark-appearing chemisorbed state (26). The rate of change in the number of precursor molecules can be expressed as  $dN_p/dt = -\nu N_p \exp(-E_b/kT_s)$ , where  $N_p$  is the coverage of precursor molecules,  $\nu$  is the pre-exponential,  $T_s$  is the substrate temperature, and  $E_b$  is the barrier to chemisorption from the precursor state. From the measured change in precursor coverage with time from successive images at  $95$  K (Fig. 4) and assuming a preexponential of  $10^{13} \text{ s}^{-1}$ , an activation barrier of  $E_b = 0.30 \pm 0.03$  eV can be deduced.

Chemisorbed benzene is known to have an adsorption energy  $E_c = 0.95 \pm 0.02$  eV (16, 18, 19, 27). From TDS measurements (16, 18) and assuming a preexponential of  $10^{13} \text{ s}^{-1}$ , an adsorption energy  $E_p \sim 0.4$  eV can be calculated for the physisorbed state. Taken together with the barrier measurement of this work, these numbers provide a full description of the energetics of this precursor-mediated chemisorption system, within the context of the model depicted in Fig. 1.

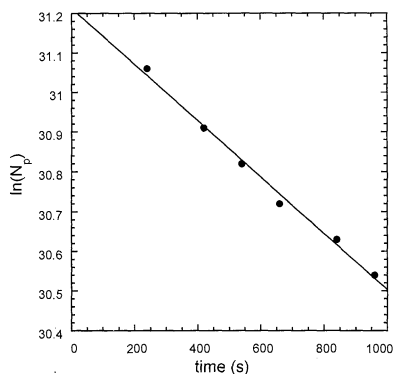


**Fig. 4.** Plot showing the decrease in the number of benzene molecules in the precursor state with time.  $N_p$  is the number of precursor molecules per square centimeter. Analysis of the data yields  $E_b = 0.30 \pm 0.03$  eV.

Free lateral motion is held to be a feature of the precursor state. The images shown, particularly those recorded at  $95$  K, indeed suggest motion; the noisy, speckled appearance of the precursors is a signature of adsorbate motion during image acquisition (28). However, this lateral precursor motion is not equally free in all directions. The most obvious indication is the strong preference of precursors to reside over center adatoms. Residence over corner adatoms probably occurs but is relatively unstable. This inference is supported by the observation that decay to the chemisorbed state results in corner adatom adsorption in only about 25% of observed transitions. Perhaps the observation that precursor motion is not entirely isotropic in this case should not come as a surprise. The expectation of unrestricted motion comes from consideration of metal surfaces that have more weakly corrugated potential energy surfaces than do semiconductors. Even though the precursor is bound by van der Waals interactions, which are by nature only weakly directional, these interactions should still be modulated by the local charge density presented by the surface. On Si(111)- $7 \times 7$  this is evidently a significant effect.

An indication of the role of the precursor state in a different temperature regime may be found in an earlier study (19) of the desorption and diffusion of molecular benzene on Si(111)- $7 \times 7$  at room temperature. The key results were that benzene experiences a very large barrier to diffusion, approximately equal to the barrier to desorption, and that diffusing molecules were often found to move to sites beyond nearest neighbors. These results can be understood in the context of our low-temperature STM results. The high diffusion barrier implies that the molecule breaks its chemical bond with the surface in order to diffuse. Evidently it enters into the precursor state, whereupon it can move laterally until either desorption or chemisorption occurs.

## REFERENCES AND NOTES

1. I. Langmuir, *Chem. Rev.* **6**, 451 (1929).
2. J. E. Leonard-Jones, *Trans. Faraday Soc.* **18**, 333 (1932).
3. For reviews of these studies, see D. A. King, in *Critical Reviews in Solid State and Materials Sciences*, D. E. Schuele and R. W. Hoffman, Eds. (CRC Press, Boca Raton, FL, 1978), vol. 7, pp. 167–208; C. R. Arumainayagam and R. J. Madix, *Molecular Beam Studies of Gas-Surface Collision Dynamics*, S. G. Davison, Ed., vol. 38 of *Progress in Surface Science* (Pergamon, New York, 1991).
4. J. B. Taylor and I. Langmuir, *Phys. Rev.* **44**, 423 (1933).
5. J. A. Becker and C. D. Hartman, *J. Phys. Chem.* **57**, 157 (1953); G. J. Ehrlich, *ibid.* **60**, 1388 (1956).
6. J. L. Morrison and J. K. Roberts, *Proc. R. Soc. London Ser. A* **173**, 1 (1939).
7. P. Kisliuk, *J. Phys. Chem. Solids* **3**, 95 (1957).
8. D. A. King and M. G. Wells, *Proc. R. Soc. London Ser. A* **339**, 245 (1974); P. Ainot and D. A. King, *Surf. Sci.* **126**, 359 (1983); C. T. Rettner, H. Stein, E. K. Schweizer, *J. Chem. Phys.* **89**, 3337 (1988); S. L. Tang, J. D. Beckerle, M. B. Lee, S. T. Ceyer, *ibid.* **84**, 6488 (1986); M. J. Grunze *et al.*, *Surf. Sci.* **139**, 109 (1984); M. P. D'Evelyn, H. P. Steinruck, R. J. Madix, *ibid.* **180**, 47 (1987); J. D. Beckerle, Q. Y. Yang, A. D. Johnson, S. T. Ceyer, *ibid.* **195**, 77 (1988).
9. P. Jakob and D. Menzel, *Surf. Sci.* **201**, 503 (1988).
10. T. Tatarenko and R. Ducros, *J. Chim. Phys. Phys. Chim. Biol.* **79**, 409 (1932).
11. D. J. Doren and J. C. Tully, *Langmuir* **4**, 256 (1987); *J. Chem. Phys.* **94**, 8428 (1991).
12. D. A. King, *Surf. Sci.* **64**, 43 (1977); A. Cassuto and D. A. King, *ibid.* **102**, 388 (1981); J. A. N. Filipe and G. J. Rodgers, *Phys. Rev. E* **52**, 6044 (1995); E. S. Hood, B. H. Toby, W. H. Weinberg, *Phys. Rev. Lett.* **55**, 2437 (1985); H. J. Kreuzer, *J. Chem. Phys.* **104**, 9593 (1996); T. Nordmeyer and F. J. Zaera, *ibid.* **97**, 9345 (1992).
13. R. Becker and R. Wolkow, in *Methods of Experimental Physics*, R. Celotta and T. Lucatorto, Eds. (Academic Press, Boston, 1993), vol. 27, pp. 149–224.
14. In addition to 12 adatoms per unit cell, there are six "rest atoms" that are not visible in the images. The role of these atoms is not central to this study (R. A. Wolkow, unpublished data).
15. M. K. Kelly *et al.*, in *Proceedings of the 17th International Conference on the Physics of Semiconductors*, J. D. Chadi and W. A. Harrison, Eds. (Springer-Verlag, New York, 1985), pp. 109–112.
16. C. D. MacPherson, D. Q. Hu, K. T. Leung, *Solid State Commun.* **80**, 217 (1991).
17. M. N. Piancastelli, R. Zanoni, J. E. Bonnet, K. Hricovini, *J. Electron Spectrosc. Related Phenomena* **68**, 383 (1994).
18. Y. Taguchi, M. Fujisawa, M. Nishijima, *Chem. Phys. Lett.* **178**, 363 (1991).
19. R. A. Wolkow and D. J. Moffatt, *J. Chem. Phys.* **103**, 10696 (1995).
20. T. E. Fischer, S. R. Kelemen, H. P. Bonzel, *Surf. Sci.* **64**, 157 (1977); R. F. Lin, R. J. Koestner, M. A. van Hove, G. A. Somorjai, *ibid.* **134**, 161 (1983); G. D. Waddill and L. L. Kesmodel, *Phys. Rev. B* **31**, 4940 (1985).
21. Two STMs were used: a homemade variable-temperature cryogenic STM [R. A. Wolkow, *Rev. Sci. Instrum.* **63**, 4049 (1992)] and a commercial Omicron instrument.
22. R. A. Wolkow and Ph. Avouris, *Phys. Rev. Lett.* **60**, 1049 (1988).
23. Molecules were leaked into the chamber and allowed to interact with the surface. Typical dosing conditions were  $10$  s at  $10^{-6}$  torr benzene pressure. When the gas leak valve was closed, vacuum pumps very quickly removed residual gaseous molecules. Therefore, virtually no adsorption events occurred during image acquisition.
24. Two mechanisms can lead to the appearance of physisorbed molecules in STM images. The first, a physical mechanism, acts when nonresonant states cause a lowering of the local barrier and hence an increased transmission coefficient [J. W. Gadzuk, *J. Appl. Phys.* **41**, 286 (1970)]. The second, a chemical mechanism, involves mixing and broadening of surface and molecule-derived states. Related effects have been seen in STM images of Xe on Ni [D. M. Eigler, P. S. Weiss, E. K. Schweizer, N. D. Lang, *Phys. Rev. Lett.* **66**, 1189 (1991)].
25. Ph. Avouris *et al.*, *Surf. Sci.* **363**, 368 (1996); J. A. Stroscio and D. M. Eigler, *Science* **254**, 319 (1991); J. A. Stroscio, L. J. Whitman, R. A. Dragoset, R. J. Celotta, *Nanotechnology* **3**, 133 (1992); L. J. Whitman, J. A. Stroscio, R. A. Dragoset, R. J. Celotta, *Science* **251**, 1206 (1991).
26. Precursor decay was observed to occur at the same rate whether an area was scanned repeatedly or infrequently. This indicates that the act of scanning plays no important role in the decay to chemisorption.
27. Y. Taguchi, M. Fujisawa, T. Takaoka, T. Okada, M. Nishijima, *J. Chem. Phys.* **95**, 6870 (1991).
28. S. J. Stranick, M. M. Kamna, P. S. Weiss, *Science* **266**, 99 (1994).
29. We thank G. P. Lopinski, S. N. Patitsas, D. D. M. Wayner, and J. C. Tully for helpful discussions. This is NRCC document 40839.

9 September 1997; accepted 21 November 1997